

Simulation of Intensity of Segregation Distributions Using Three-Dimensional FEM Analysis: Application to Corotating Twin Screw Extrusion Processing

ADENIYI LAWAL and DILHAN M. KALYON*

Highly Filled Materials Institute, Chemistry and Chemical Engineering Department, Stevens Institute of Technology, Castle Point on the Hudson, Hoboken, New Jersey 07030

SYNOPSIS

The corotating twin screw extrusion flow is simulated to generate the distributions of intensity of segregation and integral measures of mixing and forwarding. The simulation focused on the lenticular kneading disk elements that necessitated the application of a three-dimensional finite element method to solve the conservation equations. The intensity of segregation distributions were determined by introducing a tracer blob numerically and tracking the concentration of the tracer particles as a function of location and time. In spite of the chaotic nature of the dynamics of this flow, the analyses provided the broad features of twin extrusion flow and its ability to mix. The processing characteristics of kneading disks were found to depend on the stagger angle and complemented earlier numerical and experimental results on residence time distributions and color incorporated tracer analyses. © 1995 John Wiley & Sons, Inc.

INTRODUCTION

Mixing of the liquid and solid ingredients of a formulation is an important unit operation in various industrial processes including blending, compounding, and reactive processing. The mixing operation may be extensive (distributive) or intensive (dispersive) in character.¹⁻³ Distributive mixing involves the interspersing in space of two or more components; dispersive mixing describes a multitude of processes in which some intrinsic change takes place in the physical character of one or more components. The change in the particle size distribution of a solid component during mixing is a typical example of a dispersive process. In spite of recent advances in theory and simulation made in this area,⁴⁻⁶ industrial mixing is currently an art rather than a science.

The efficiency and "quality" of the mixing operation directly affect the ultimate properties of articles manufactured using the mixing step. The major challenge in advancing the quality of the mixing

operation stems from the difficulties involved in establishing quantitative and measurable indices to describe the degree of mixing on a case by case basis. The industry generally relies on indirect measures of mixture quality that incorporate transmissive, reflective, resistivity, ultrasound, and rheological measurements. Such indirect techniques furnish little insight on the prevailing mechanism of mixing and the experimental results cannot be related to numerical data obtained upon simulation of the dynamics of the mixing operation.⁵⁻⁷

Direct and quantitative characterization of the "degree of mixedness" is possible if experimental means are available to determine the spatial concentration distributions of one or more of the components at various stages of the mixing operation. Such experiments can be carried out at the desired scale of examination.¹ The degree of mixedness then can be characterized by the statistical analyses of the concentration distributions. Mixing indices can be defined by the comparison of the variance of the experimental concentration distribution to those of the binomial distribution (random mixing) or completely segregated systems. The intensity of segregation⁸ defined as the ratio of the variance of

* To whom correspondence should be addressed.

the concentration values over the variance of the segregated system is widely used. It has been applied to the mixing analyses of color tracer incorporated thermoplastic elastomers⁹ and concentrated suspensions.¹⁰

The availability of experimental techniques to characterize the distribution of intensity of segregation renders its use in simulation studies of mixing very attractive. In this article, new simulation techniques that can map out the distributions of intensity of segregation as a function of geometry, and operating conditions of the mixer are presented. The simulation technique is applied to the corotating twin screw extruder, that is, a widely used and versatile continuous processor. However, the techniques are equally applicable to other batch and continuous mixers.

The methodology is applied to the most difficult to simulate elements of the corotating twin screw extrusion process, that is, the kneading disk elements staggered forward at various angles. The intensity of segregation distribution of a passive, non-diffusive tracer as a function of screw geometry is considered.

ANALYSIS

Flow Equations

The kneading disk screw elements of the fully intermeshing corotating twin screw extruder are shown in Figure 1. The flow in such elements occurs on the basis of the calendaring action between the two screws and the screw and barrel sections. As shown in Figure 2, regions of forward and reverse squeezing flows (flow occurring in $+z$ and $-z$ directions) occur simultaneously. The velocity distribution changes rapidly, dependent on the orientations

of the kneading paddles within each period of rotation.⁷ The demonstrated three-dimensional (3-D) nature of the flow field and the presence of a relative velocity between the two screws render this method more realistic in comparison to the unwrapping of the screw channel, a popular approach in twin screw extrusion analysis.^{11,12}

The conservation equations for the 3-D flow problem in the kneading block areas are given below. Here, u_x , u_y , and u_z are velocity components in x , y , and z directions. τ_{ij} is the ij component of the stress tensor and P is pressure.

$$\frac{\partial u_x}{\partial x} + \frac{\partial u_y}{\partial y} + \frac{\partial u_z}{\partial z} = 0 \quad (1)$$

$$\frac{\partial P}{\partial x} = \left(\frac{\partial \tau_{xx}}{\partial x} + \frac{\partial \tau_{yx}}{\partial y} + \frac{\partial \tau_{zx}}{\partial z} \right) \quad (2)$$

$$\frac{\partial P}{\partial y} = \left(\frac{\partial \tau_{xy}}{\partial x} + \frac{\partial \tau_{yy}}{\partial y} + \frac{\partial \tau_{zy}}{\partial z} \right) \quad (3)$$

$$\frac{\partial P}{\partial z} = \left(\frac{\partial \tau_{xz}}{\partial x} + \frac{\partial \tau_{yz}}{\partial y} + \frac{\partial \tau_{zz}}{\partial z} \right). \quad (4)$$

The conservation equations are solved with no-slip conditions at the barrel and rotating screw surfaces. For the discretization of eqs. (1)–(4) the penalty/Galerkin finite element method is employed. The continuity equation is considered as a constraint on equations of conservation of momentum and the pressure, P , is approximated by using a large positive number, β_p (penalty parameter):

$$P = -\beta_p \eta \left(\frac{\partial u_x}{\partial x} + \frac{\partial u_y}{\partial y} + \frac{\partial u_z}{\partial z} \right). \quad (5)$$

where η is the dimensionless shear viscosity.

A single finite element method (FEM) mesh is necessary¹³ and the locations occupied by the solid disks and fluid are governed by the positions of the

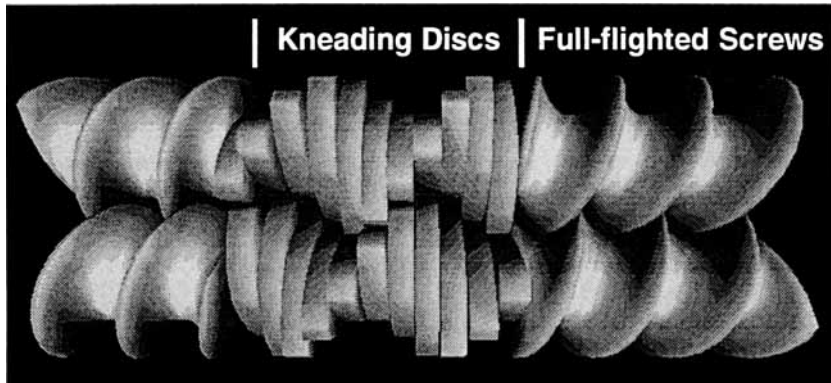


Figure 1 Various screw elements of corotating twin screw extruder.

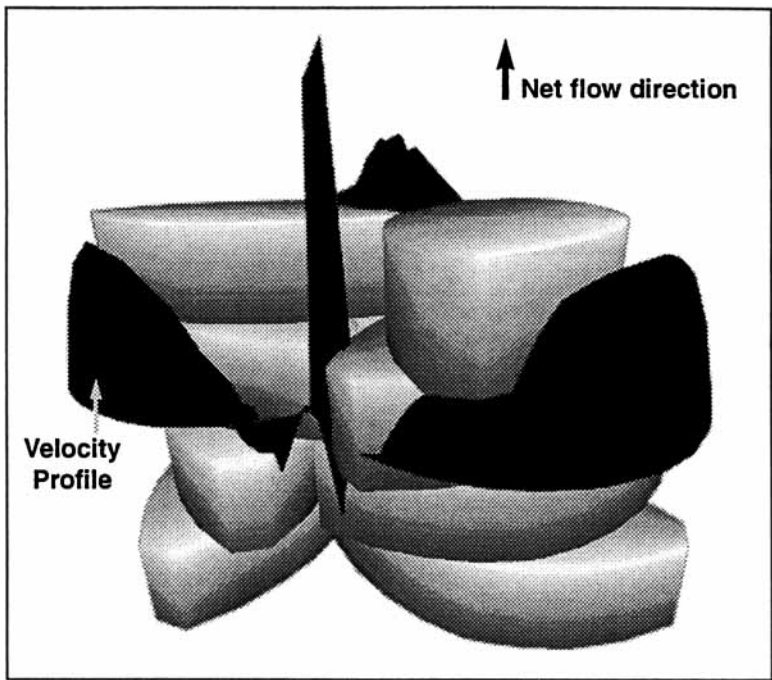


Figure 2 Typical instantaneous distribution of dimensionless axial velocity component (u_z^*) at the kneding disk section for disks staggered at 30° forward. $u_z^* = u_z/R_s\omega$ where R_s is the barrel diameter and ω is the screw rotational speed in radians/second.

kneading disk pair that change as a function of time during each period of rotation. For each period 36 configurational positions, 10° apart, are considered, eqs. (2)–(4) were then solved to determine the time-dependent velocity distributions.^{5-7,13} With the Eulerian velocity field determined, the trajectory $\mathbf{x} = \mathbf{x}(\mathbf{X}, t)$ of a fluid particle initially located at a point \mathbf{X} is obtained following the tracking procedures that we developed earlier.^{5-7,14}

Representative isothermal results will be presented here for two-tipped lenticular kneding disk elements. The four stagger angles considered are 30° , 45° , and 60° forward and 90° neutral. The equations were rendered dimensionless by the use of the barrel radius for distance, rotational speed of the kneding disks for velocity and time, and the viscosity of the Newtonian fluid and screw speed for pressure.⁵⁻⁷ All operating conditions and geometry, except for the stagger angle, were kept the same to facilitate a fair comparison of the effects of stagger angle of the kneding disks on the intensity of segregation distributions.

Mixing Index

The most complete mixing state attainable by a mixture corresponds to the statistical randomness

of the ultimate particles of the components being mixed in all the different regions of the mixture, that is, binomial distribution. As indicated earlier the extent to which the concentration in the various regions of the mixture deviates from the mean concentration, that is, the variance s^2 , is an indication of the degree of homogeneity of the mixture.

For the purpose of our analysis, we imagine the mixture to be divided into different regions of approximately equal volume, with this volume defining the scale of examination. The s^2 of the mixture is then given by:

$$s^2 = \frac{\sum_{i=1}^N V_i (X_i - \bar{X})^2}{\sum_{i=1}^N V_i} \tag{6}$$

where V_i is the volume of each region, X_i is the concentration of the component of interest in each region, \bar{X} is the mean concentration, and N is the number of different regions. A small variance indicates a homogeneous system. The variance is maximum when the components are completely segregated, that is,

$$s_{\text{seg}}^2 = \bar{X}(1 - \bar{X}). \tag{7}$$

The intensity of segregation I_v , of a mixture is the ratio of the variance of the mixture, s^2 , to the variance of the completely segregated mixture, s_{seg}^2 , both defined at the same mean concentration:

$$I_v = s^2 / s_{\text{seg}}^2. \quad (8)$$

The value of the intensity of segregation varies from unity for a completely segregated system, to zero for an ideal homogeneous system.

To determine the intensity of segregation using numerical simulation, we placed a blob of nondiffusive tracer at an initial location found at the entrance of the kneading block section of the extruder. Using the tracking technique, we followed its spreading for a certain duration of time measured in periods of revolution of the kneading disk elements of the extruder. Specifically, a blob of dimensionless radius of 0.08, which is made up of 17,227 discrete particles, is located initially at the dimensionless location of $x = 0.775$, $y = 0.775$, and $z = 0.1$. Between any two axial cross-sectional planes of the extruder, there are finite elements that serve as the scale of examination. At each cross-sectional area the values of the concentration of the tracer in each element and the mean concentration are determined from the following equations:

$$X_i = \frac{\text{no. of tracer particles in each finite element}}{\text{total no. tracer particles at axial cross-sectional region}} \quad (9)$$

$$\bar{X} = \frac{\sum_{i=1}^N X_i V_i}{V_f} \quad (10)$$

where N is the number of finite elements in the axial cross-sectional region, and V_f is the total free volume available to the particles between the two cross-sectional planes. Notice that $\sum_{i=1}^N X_i$ will add up to one as required and that the free volume V_f should replace $\sum_{i=1}^N V_i$ in eq. (6), because some of the finite elements are occupied by the kneading disks.

After making the appropriate substitutions, I_v becomes:

$$I_v = \frac{\sum_{i=1}^N V_i X_i^2 - \bar{X} \sum_{i=1}^N X_i V_i}{(1 - \bar{X}) \bar{X} V_f} \quad (11)$$

and the intensity of segregation at each axial cross-sectional region of the extruder can thus be calculated at the desired time of interest. From this an axially averaged intensity of segregation, \bar{I}_v , can be obtained:

$$\bar{I}_v = \frac{\int_{z_i}^{z_f} I_v z dz}{\int_{z_i}^{z_f} z dz} \quad (12)$$

where z_i is the initial axial location where the particles are detected and z_f is the final location where significant presence of particles is encountered. The axially averaged intensity of segregation is similar to the integral distance weighted mixing index defined by Kalyon and Sangani⁹ to represent the mixing achieved over the entire continuous mixer for the total down-channel distance ($z_f - z_i$). Experimental results with incorporated color tracer indicated that the integral distance weighted mixing index for a stagger angle of 90° is significantly smaller than those at forward configurations.⁹ This suggests a more efficient distributive mixing process with the 90° stagger angle in comparison to kneading disks staggered in forward configuration. Finally, the average degree of the forwarding capability of the kneading disk configurations can be determined by employing the forwarding index, \bar{z} (Kalyon and Sangani⁹):

$$\bar{z} = \frac{\int_{z_i}^{z_f} \bar{X}(z) z dz}{\int_{z_i}^{z_f} \bar{X} dz} \quad (13)$$

where $\bar{X}(z)$ is the mean concentration of tracer particles at the cross section located at axial distance z . Previous experimental twin screw extrusion results have shown that the forwarding indices for the kneading disks staggered at forward configurations are greater than those of the neutral and reversely configured kneading disks.⁹

RESULTS AND DISCUSSION

Figure 3 shows the axial distribution of the intensity of segregation (I_v) after seven periods of revolution of the kneading disks, staggered forward at the four different stagger angles considered in this study. One observes that, in the middle portion of the extruder,

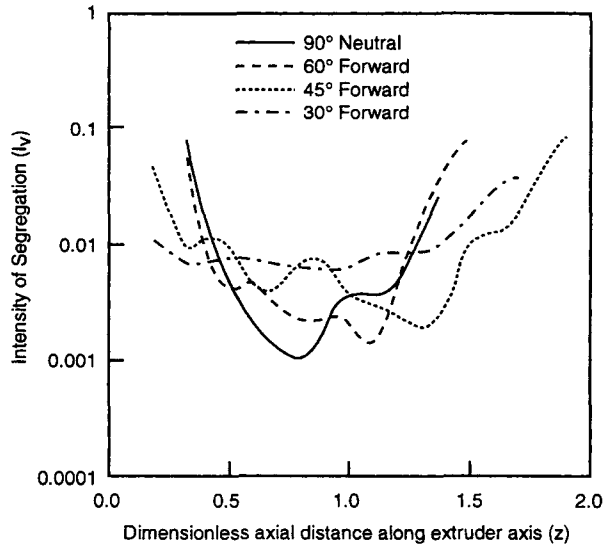


Figure 3 The axial distributions of the intensity of segregation (I_v) for different forward stagger angle configurations at seven periods.

where most of the discrete particles are located at the end of the seven periods of screw rotation, the high stagger angle configurations exhibit lower values of the intensity of segregation, indicative of better homogeneity. As time elapses the same pattern persists as demonstrated in Figure 4 for 10 periods of revolution. Comparison of Figures 3 and 4 indicates that the intensity of segregation values decrease with time. From such numerical experimen-

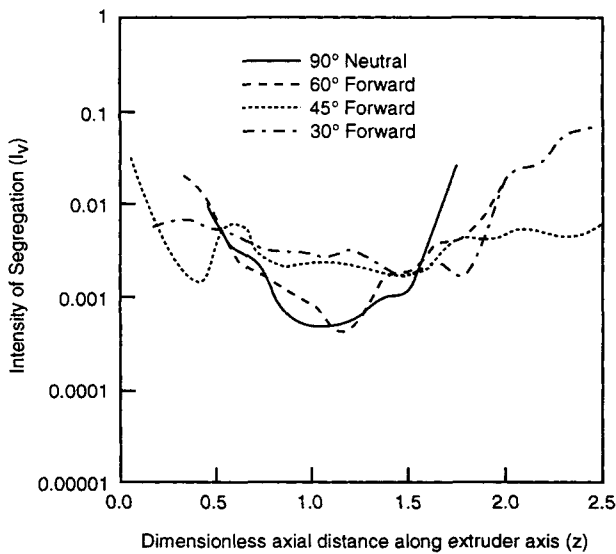


Figure 4 The axial distributions of the intensity of segregation (I_v) for different forward stagger angle configurations of kneading disks at 10 periods.

tation, one can determine the optimum number of periods of revolution for achieving the desired value of the intensity of segregation.

The axially averaged intensity of segregation as a function of the number of periods for the various stagger angles is shown in Figure 5. Consistently again, the high stagger angle configurations display lower values of intensity of segregation. While the 30° and 90° stagger angles seem to have reached a plateau at about 10 periods, the 45° and 60° stagger angle configurations will require a longer duration of processing to achieve the minimum value of I_v for the conditions considered in the present case study. These results also show why it is so difficult to obtain reliable experimental data with color incorporated tracers that can be scaled up. Color incorporated tracers can only be identified to generate mixing indices if the blobs incorporated into the mixture remain coherent. This is only possible at a small number of periods of rotation. However, as shown in Figure 5, the relative mixing behavior obtained at relatively small number of periods will generate misleading results when extrapolated to a greater number of periods, consistent with industrial mixing practice. This emphasizes why it is so important to be able to generate experimental results in mixing directly from the materials of interest,^{10,15} and under the actual geometry and operating conditions.

Finally, as shown in Figure 6, the lower stagger angle configurations, that is, 30° and 45°, have higher forwarding index, \bar{z} , values in comparison

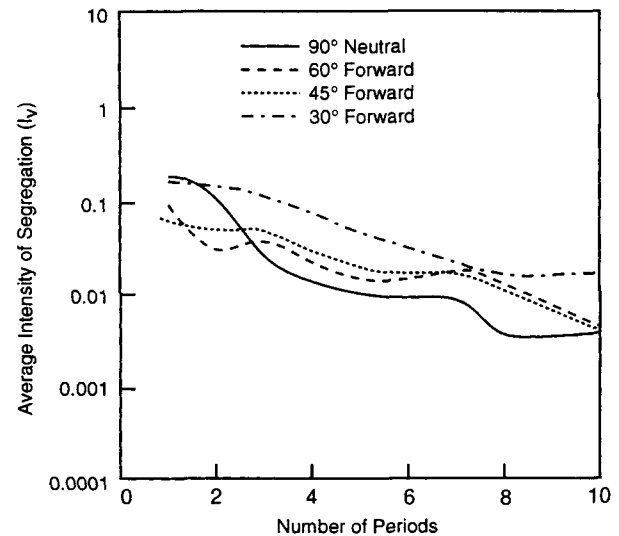


Figure 5 The axially averaged intensity of segregation (\bar{I}_v) as a function of the number of periods of revolution of the kneading disk elements.

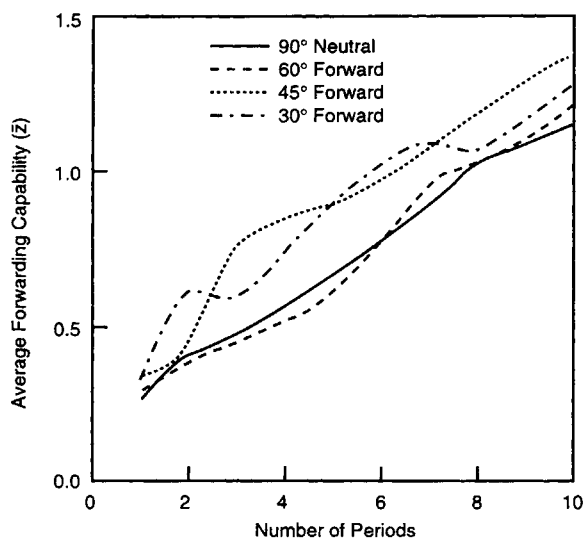


Figure 6 The average forwarding index (\bar{z}) as a function of the number of periods of revolution of the kneading disk elements.

with the configurations with greater stagger angles. Furthermore, the forwarding index increases with time as one would expect for the kneading disks staggered in the forward direction.

These results complement our earlier numerical and experimental findings on twin screw extrusion flow generated by kneading disks.^{6,7,9,16} The motion generated by the kneading disks was shown to be governed by chaotic dynamics characterized by the rapid divergence of initial conditions.⁷ Kneading disks configured with small stagger angles were shown to generate a broader distribution of residence times with both channeling (small residence times) and stagnation (long residence times) in comparison to disks staggered at greater stagger angles.⁷ Furthermore, regions of segregated flow (completely unmixed regions) could be observed for the 30° stagger angle.⁹

The intensity of segregation distributions and integral measures of mixing and forwarding reported in Figures 3–6 support these earlier findings. The greater forwarding ability of the kneading disks with smaller stagger angles occurs at the expense of the deterioration of the degree of mixedness, that is, greater values of intensity of segregation. Furthermore, greater forwarding capability of smaller stagger angles should be associated with their greater pressurization capability at equal volumetric flow rate. Earlier studies have indeed indicated that pressurization capability increases with decreasing stagger angles.¹⁶

CONCLUSIONS

Techniques to simulate the degree of mixedness distributions were developed and applied to the kneading disk section of the corotating twin screw extruder. Numerical tracer analysis using the intensity of segregation parameters provided a quantitative measure of the mixing quality. The intensity of segregation distributions can also be characterized experimentally and thus, for the first time, it becomes possible to determine and compare the degree of mixedness distributions generated by industrial mixers simultaneously both theoretically and experimentally. For the four forward stagger angles and the set of conditions utilized here, the value of the intensity of segregation decreases with increased stagger angle of the lenticular kneading disk elements to give rise to better distributive mixing. The forwarding index increases with decreasing stagger angle, suggesting a greater pressurization capability. These results complement earlier experimental and theoretical findings that indicated that smaller stagger angles generate broader residence time distributions and regions of unmixed, segregated flow. The results further attest to the nonlinear nature of the flow field and emphasizes the importance of simulation or experimental characterization of mixing only under conditions that mimic the industrial operation of interest.

This research has been sponsored by BMDO/IST as managed by Dr. Richard S. Miller of ONR (Grant Number N00016-86-K-0620), for which we are grateful. The content of the information does not necessarily reflect the position or the policy of the Government, and no official endorsement should be inferred.

REFERENCES

1. J. M. McKelvey, *Polymer Processing*, Wiley, New York, 1962.
2. Z. Tadmor and C. G. Gogos, *Principles of Polymer Processing*, Wiley, New York, 1979.
3. D. M. Kalyon, *Handbook of Polymer Science and Technology*, Vol. 3, N. D. Cheremisinoff, Ed., Marcel Dekker, New York, 1989, Chap. 8.
4. J. M. Ottino, *The Kinematics of Mixing: Stretching, Chaos and Transport*, Cambridge University Press, Cambridge, UK, 1989.
5. A. Lawal, D. M. Kalyon, and Z. Ji, *Polym. Eng. Sci.*, **33**, 140–148 (1993).
6. A. Lawal and D. M. Kalyon, *SPE ANTEC Tech. Pap.*, **39**, 3397–3400 (1993).

7. A. Lawal and D. M. Kalyon, *Polym. Eng. Sci.*, **35**, 1325 (1995).
8. P. V. Danckwerts, *Appl. Sci. Res.*, **3A**, 279 (1952).
9. D. M. Kalyon and H. N. Sangani, *Polym. Eng. Sci.*, **29**, 1018 (1989).
10. R. Yazici and D. M. Kalyon, *Rubber Chem. Technol.*, **66**, 527 (1993).
11. W. Szydlowski, R. Brzoskowski, and J. L. White, *Int. Polym. Proc.*, **1**, 207 (1987).
12. W. Szydlowski and J. L. White, *Int. Polym. Proc.*, **2**, 142 (1988).
13. A. D. Gotsis, Z. Ji, and D. M. Kalyon, *SPE ANTEC Tech. Pap.*, **36**, 139 (1990).
14. D. M. Kalyon, A. D. Gotsis, U. Yilmazer, C. G. Gogos, H. Sangani, B. Aral, and C. Tsenoglou, *Adv. Polym. Technol.*, **8**, 337 (1988).
15. D. M. Kalyon, R. Yazici, C. Jacob, B. Aral, and S. W. Sinton, *Polym. Eng. Sci.*, **31**, 1386 (1991).
16. D. M. Kalyon, C. Jacob, and P. Yaras, *Plast. Rubber Comp. Proc. Applications*, **16**, 193 (1991).

Received November 28, 1994

Accepted May 30, 1995